

1 **A Fast-response automated gas equilibrator (FaRAGE) for continuous *in situ***
2 **measurement of CH₄ and CO₂ dissolved in water**

3 Shangbin Xiao¹, Liu Liu^{2*}, Wei Wang¹, Andreas Lorke^{1,3}, Jason Woodhouse² and Hans-Peter
4 Grossart^{2,4*}

5 ¹ College of Hydraulic & Environmental Engineering, China Three Gorges University, 443002 Yichang, China

6 ² Department of Experimental Limnology, Leibniz Institute of Freshwater Ecology and Inland Fisheries, 16775
7 Stechlin, Germany

8 ³ Institute for Environmental Sciences, University of Koblenz-Landau, 76829 Landau, Germany

9 ⁴Institute of Biochemistry and Biology, Potsdam University, 14669 Potsdam, Germany

10 *Corresponding authors

11 Emails: liu.liu@igb-berlin.de; hgrossart@igb-berlin.de

12 **Abstract**

13 Biogenic greenhouse gas emissions, e.g. of methane (CH₄) and carbon dioxide (CO₂)
14 from inland waters contribute substantially to global warming. In aquatic systems, dissolved
15 greenhouse gases are highly heterogeneous both in space and time. To better understand the
16 biological and physical processes that affect sources and sinks of both CH₄ and CO₂, their
17 dissolved concentrations need to be measured with high spatial and temporal resolution. To
18 achieve this goal, we developed the **Fast-Response Automated Gas Equilibrator (FaRAGE)**
19 for real-time *in situ* measurement of dissolved CH₄ and CO₂ concentrations at the water surface
20 and in the water column. FaRAGE can achieve an exceptionally short response time ($t_{95\%} = 12$
21 s when including the response time of the gas analyzer) while retaining an equilibration ratio
22 of 62.6% and a measurement accuracy of 0.5% for CH₄. A similar performance was observed
23 for dissolved CO₂ ($t_{95\%} = 10$ s, equilibration ration 67.1%). An equilibration ratio, as high as

24 91.8%, can be reached at the cost of a slightly increased response time (16 s). The FaRAGE is
25 capable of continuously measuring dissolved CO₂ and CH₄ concentrations in the nM-to-sub mM
26 (10⁻⁹ - 10⁻³ mol L⁻¹) range with a detection limit of sub-nM (10⁻¹⁰ mol L⁻¹), when coupling with
27 a cavity ring-down greenhouse gas analyzer (Picarro GasScouter). FaRAGE allows for the
28 possibility of mapping dissolved concentration in a “quasi” three-dimensional manner in lakes
29 and provides an inexpensive alternative to other commercial gas equilibrators. It is simple to
30 operate and suitable for continuous monitoring with a strong tolerance to suspended particles.
31 While the FaRAGE is developed for inland waters, it can be also applied to ocean waters by
32 tuning the gas-water mixing ratio. The FaRAGE is easily adapted to suit other gas analyzers
33 expanding the range of potential applications, including nitrous oxide and isotopic composition
34 of the gases.

35 **1 Introduction**

36 Despite the well-established perception of inland waters as a substantial source of
37 atmospheric methane (CH₄) and carbon dioxide (CO₂) (Bastviken et al., 2011; Cole et al., 2007;
38 Tranvik et al., 2009), the magnitude of these greenhouse gases remains uncertain owing to the
39 fact that some key processes affecting CH₄ (e.g. bubbling) and CO₂ budget are still poorly
40 constrained (Saunois et al., 2019). Most freshwater lakes and reservoirs are often oversaturated
41 with CH₄ and CO₂ (relative to atmosphere) and their distribution are characterized by high
42 spatio-temporal heterogeneity (Hofmann, 2013). Point-based and short-term measurements can
43 result in biases in estimating diffusive CH₄ flux (Paranaíba et al., 2018). Thus, resolving the
44 spatio-temporal dynamics of both dissolved CH₄ and CO₂ is a prerequisite for a better
45 understanding of production and loss processes of these gases in freshwater lakes.

46 The distribution of CH₄ and CO₂ in lakes is often characterized by pronounced vertical
47 and horizontal concentration gradients, which often coincides with the position of the
48 thermocline. In many deep stratified lakes, a sharp vertical gradient of CH₄, for instance, below
49 the thermocline can develop in the anoxic hypolimnion (mM range) (Encinas Fernández et al.,
50 2014; Liu et al., 1996). In contrast, in some stratified lakes with a fully oxygenated hypolimnion
51 CH₄ can accumulate above the thermocline (~µM range) (Grossart et al., 2011; Donis et al.,
52 2017; Günthel et al., 2019). In addition to formation processes that lead to CH₄ accumulation,
53 the concentration of dissolved CH₄ is also regulated by losses due to oxidation and emission to
54 the atmosphere (Bastviken et al., 2004; Juutinen et al., 2009). Emission rates, in particular, are
55 highly variable dependent on turbulence induced by wind or convective mixing (Read et al.,
56 2012; Vachon and Prairie, 2013). Vertical distributions of CH₄ and CO₂ can be further
57 confounded the contribution of littoral sediments which can result in distinct horizontal
58 gradients of CO₂ and CH₄ (Murase et al., 2003). Accounting for horizontal gradients is therefore
59 critical as lateral transport may account for a proportion of the epilimnetic CH₄ peak observed

60 in pelagic waters via (Hofmann et al., 2010; Fernández et al., 2016; Murase et al., 2005; Peeters
61 et al., 2019).

62 Spatial distributions of CH₄ and CO₂ in aquatic systems, vary over time, particularly as
63 factors which control their production, consumption and loss to the atmosphere fluctuate.
64 Concentrations of CH₄ and CO₂ in lakes demonstrate profound seasonality, driven primarily by
65 thermal stratification (Encinas Fernández et al., 2014) and phytoplankton dynamics (Günthel et
66 al., 2019). While the build-up of hypolimnetic CH₄ storage is a slow process that is closely
67 related to the development of lake hypoxia, epilimnetic CH₄ and CO₂ can be highly variable
68 even at a daily basis as they are strongly affected by phytoplankton dynamics (Günthel et al.,
69 2019; Hartmann et al., 2020; Bižić et al., 2020). In addition, storms can act as another driver
70 for short-term dissolved gas dynamics in the lake because they often contribute to higher
71 evasion rates caused by strong vertical turbulent mixing (Zimmermann et al., 2019) and
72 enhanced horizontal transport (Fernández et al., 2016). While the seasonal patterns of dissolved
73 CH₄ and CO₂ concentration in lake water seem recurrent and can be simulated (Stepanenko et
74 al., 2016), the unpredictable effects of short-term biological dynamics and storm events can
75 present a challenge in modeling the dynamics of greenhouse gases in lakes.

76 While there is an urgent need for resolving the spatio-temporal variability of CH₄ in
77 large water bodies (e.g. lakes), we recognize limitations in the available methodology. Like
78 most gases in dissolved phase, CH₄ and CO₂ cannot be measured directly in water. Instead, a
79 carrier gas (synthetic air or at air concentration) is added to achieve (full/partial) gas-water
80 equilibration. The headspace gas sample is then measured with a gas spectrometer and the
81 concentration of targeted gas can be calculated according to Henry's law (Magen et al., 2014).
82 To save sampling effort, continuous gas equilibration devices have been developed, which
83 generally can be classified in four categories: 1) Membrane type (Schlüter and Gentz, 2008;
84 Boulart et al., 2010; Gonzalez-Valencia et al., 2014; Hartmann et al., 2018) - gases are extracted

85 from water using a gas-permeable membrane; 2) Marble type (Frankignoulle et al., 2001;
86 Santos et al., 2012) - gas exchange is enhanced by pumping water through marbles that
87 increases the gas-water contact area; 3) Bubble type (Schneider et al., 1992; Körtzinger et al.,
88 1996; Güllow et al., 2011) - dissolved gases are stripped out by bubbling the water sample; 4)
89 Showerhead type (Weiss-type) (Johnson, 1999; Rhee et al., 2009; Li et al., 2015) - water is
90 pumped from top and then mixed with a circulated headspace carrier gas. A full evaluation on
91 the performance of these devices was provided in a recent review (Webb et al., 2016), where,
92 the most important parameter, response time, was found to vary between 2-34 min for
93 dissolved CH₄. While it is already encouraging, improvements are expected to further shorten
94 the response time.

95 Driven by the need to resolve temporal and spatial variability of dissolved CH₄ and CO₂
96 in inland waters with sufficient precision, we developed a novel, low-cost equilibrator to
97 achieve fast gas-water equilibration. The **Fast-Response Automated Gas Equilibrator**
98 **(FaRAGE)** can be coupled with a portable gas analyzer, which makes it perfect for field use.
99 Here, the performance of the FaRAGE is evaluated by investigating its response time, detection
100 limit and equilibration ratio. Although FaRAGE is developed for inland waters, it can be also
101 adapted for oceanographic applications. Applications are provided exemplarily to demonstrate
102 the potential of the FaRAGE for improving our understanding on the spatial distribution and
103 temporal dynamics of dissolved CH₄ and CO₂ in inland waters.

104 **2 Materials and Methods**

105 **2.1 Device description**

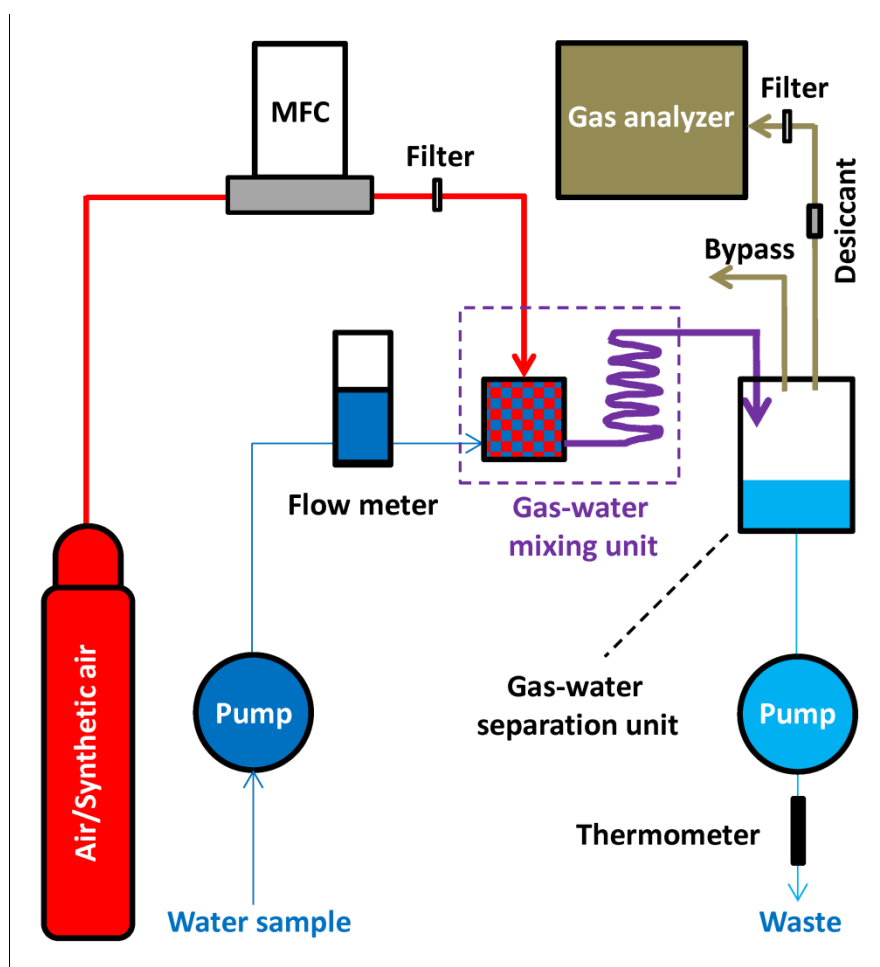
106 The design of the FaRAGE is modified from two types of equilibrators: Bubble-type
107 (Schneider et al., 1992) and Weiss-type (Johnson, 1999). In contrast to the traditional bubble-
108 type and Weiss-type equilibrators that create a large-volume headspace and circulates air back

109 to the headspace, the FaRAGE is a flow-through system that adds gas flow into a constant water
110 flow to produce a minimal headspace for continuous concentration measurement of CO₂ and
111 CH₄ dissolved in water.

112 The operation principle of the FaRAGE is depicted in Fig. 1 and technical drawings of
113 the main parts of the prototype are provided in Fig. S1. A list of information on suppliers and
114 cost of each part can be found in Table S1. A mass flow controller (SIERRA C50L, Netherlands)
115 is used to generate a constant carrier gas (normal air/synthetic air) flow (1 L min⁻¹) from a
116 compressed air tank coupled with a pressure regulator. Water samples are taken continuously
117 using a peristaltic pump (500 mL min⁻¹), and the flow is monitored using a flow meter (Brooks
118 Instrument, Germany). The two flows mix in a gas-water mixing unit and then travel through a
119 coiled hose for further gas-water turbulent mixing. In the gas-water mixing unit (modified from
120 a 10 mL plastic syringe), a jet flow is created by adapting narrowed tubing (2 mm inner diameter)
121 to the water pumping hose (3.2 mm inner diameter). Degassing occurs when the jet flow enters
122 the chamber with a sudden enlarged diameter (14 mm). Degassing is further enhanced by micro-
123 bubbles that are generated by a bubble diffusor attached to the carrier gas hose (inside the plastic
124 syringe). The gas-water mixture flows through the 2-m long Tygon tube (3.2 mm inner diameter)
125 where additional equilibration occurs. The flow is finally introduced to a gas-water separation
126 unit (a 30 mL plastic syringe) where the headspace gas is separated from the water. In this
127 chamber, water falls down freely to the bottom while the headspace gas is taken directly to a
128 greenhouse gas analyzer (1 L min⁻¹ gas pumping rate; GasScouter G4301, Picarro, USA). A 2-
129 m long Tygon tube (3.2 mm inner diameter) is attached to the top of the chamber for venting
130 excess gas flow while stabilizing gas pressure in the headspace. The bottom water is discharged
131 back to the lake using another peristaltic pump (500 mL min⁻¹). To protect the gas analyzer
132 from damaging high water vapor content, a Teflon membrane filter (pore size 0.2 μm) is placed
133 before the gas intake (resulting in a ~210 mL min⁻¹ reduction in flow rate of gas sample, which

134 is vented from the bypass at the top of the gas separation unit). A desiccant (a 20 mL plastic
135 syringe filled with dried silicone beads) is used to reduce moisture concentration when attaching
136 to a Picarro G2132-i isotope analyzer (Picarro, USA), in which < 1% moisture level is required
137 for ^{13}C -CH₄ measurement. The temperature of the water sample at the point of equilibration
138 with the headspace gas is monitored using a fast thermometer (precision 0.001 °C, 1 Hz, TR-
139 1050, RBR, Canada) attached to the end of the water discharging hose.

140 In addition to Gas Scouter from Picarro, two additional widely used models of
141 greenhouse gas analyzers were tested. They are the Ultraportable Los Gatos (Los Gatos
142 Research, USA) and stable isotopic CH₄ analyzer (G2132-i, Picarro, USA). The main technical
143 details of all three tested gas analyzers are listed in Table S2.



144

145 **Fig. 1** Schematic design of the FaRAGE. The components include: Air tank containing
146 compressed carrier gas (air or synthetic air) with a pressure regulator, a mass flow controller
147 (MFC) for generating constant carrier gas flow, two peristaltic pumps for taking and
148 discharging water, respectively, a flow meter for monitoring water sample flow, a gas-water
149 mixing unit, a gas-water separation unit, a gas analyzer, and a thermometer for measuring water
150 temperature at phase equilibration. A Teflon membrane filter is placed after the MFC and
151 another is added before the gas analyzer to protect from being flooded. A desiccant is used to
152 dry the gas flowing to the gas analyzer (if Picarro isotopic analyzer is used). The red color
153 marks the flow of carrier gas, dark blue line indicates the water sample, purple line shows the
154 flow of gas-water mixture, the light brown line shows the flow of gas sample (after partial
155 equilibration) and the light blue line depicts the water discharged back to lake. The thickness
156 of the lines scales with the gas/water flow rates. The arrows show the flow directions.

157 **2.2 Laboratory validation**

158 The FaRAGE prototype was first tested intensively in the laboratory to determine both
159 the equilibration ratio and response time. The tests were performed for both CH₄ and CO₂ with
160 a GasScouter G4301 (Picarro, USA), which measures both gases simultaneously. The
161 equilibration ratio is defined as the concentration of the gas at the outlet of the gas equilibrator
162 in comparison to the equilibrium concentration (full gas-water equilibration). The equilibration
163 ratio was established across a range of stock solutions (nano-to-milli molar dissolved gas
164 concentrations). These standard solutions were prepared by adding different amounts of either
165 CH₄ or CO₂ into a 200 mL headspace of a 2 L Schott bottle filled with Milli-Q water. The exact
166 concentrations in these solutions were tested with the manual headspace method: a 400 mL
167 headspace was created in a 500 mL plastic syringe with nitrogen gas. The gas concentration of
168 the headspace gas was then measured using GasScouter G4301. At the same time, dissolved
169 CH₄ and CO₂ concentrations of these standard solutions were measured with the FaRAGE for

170 at least 2 min and an average was calculated from more than 60 individual data points. We
171 directly compared dissolved gas concentrations measured using the two different methods, i.e.,
172 our equilibrator and manual headspace method.

173 The response time of the device was investigated by switching the water sample inlet
174 between two water samples with different concentrations of either CH₄ or CO₂. Triplicated
175 measurements were performed. An exponential fit was applied to the concentration change
176 curve and the response time was determined as time needed to reach 95% of the final
177 concentration.

178 The effect of water-to-gas mixing ratio on equilibration ratio and response time of the
179 device was investigated. By fixing the carrier gas flow rate to 1 L min⁻¹, the water-to-gas mixing
180 ratio was varied from 0.04, 0.08, 0.12, 0.15, 0.24, 0.29, 0.36, 0.43 and 0.5 by adjusting the water
181 sample flow rate. The effect of tube length on performance of the device was also examined by
182 adapting 1, 2, 4.4, 8.4 and 13 m Tygon tube onto the gas-water mixing unit. For all these tests,
183 triplicated measurements of the equilibration ratio and response time were performed
184 corresponding to different mixing ratios and the mean values were used for analysis.

185 Tests were performed to investigate the performance of the device when adapting to two
186 other types of gas analyzers. As the equilibration ratio is unaffected by the model of gas
187 analyzers, only response time was determined. This was done by fixing carrier gas and water
188 sample flow rates to 1 and 0.5 L min⁻¹, respectively. The surplus gas was vented to the air as
189 Ultraportable Los Gatos and Picarro G2132-i have a gas intake flow rate of only 500 and 25
190 mL min⁻¹, respectively. The effect of desiccant on response time of Picarro G2132-i was
191 checked by measuring gas samples with and without a desiccant installed.

192 **2.3 Field tests**

193 Four lakes in Germany were chosen for field tests. Lake Stechlin is a deep meso-
194 oligotrophic lake with a maximum depth of 68 m and Lake Arend is a eutrophic lake with a
195 maximum depth of 48 m. Pronounced CH₄ peaks in the epilimnion of Lake Stechlin have been
196 previously reported that were measured with two different methods (manual headspace method
197 in Grossart et al. (2011) and Tang et al. (2014); membrane-based gas equilibrator in Hartmann
198 et al. (2018)). This makes it ideal for our testing purpose. While CH₄ profiles at Lake Arend
199 have never been reported, the metalimnetic oxygen minimum in the lake observed during
200 summer (Kreling et al., 2017) renders it interesting for CH₄ profiling throughout the entire water
201 column. Additionally, we selected both eutrophic lakes with an anoxic hypolimnion (Lake
202 Großer Pälitz and Lake Zotzen), where CH₄ and CO₂ can accumulate during the period of
203 thermal stratification. Measurements were conducted in these two lakes to test the capability of
204 FaRAGE to measure water with high dissolved CH₄ and CO₂ concentrations.

205 Due to the high potential of the FaRAGE for real-time *in situ* measurement of dissolved
206 CH₄ and CO₂ concentrations, we explored potential field applications. These field tests included
207 depth profiling of dissolved CH₄ concentrations in the four lakes and investigations of the
208 horizontal distribution of surface dissolved CH₄ and CO₂ concentrations across the entire Lake
209 Stechlin. For the first application, a fast-response CTD (conductivity, temperature and depth)
210 profiler (XR-620 CTD+, RBR, Canada) was mounted onto a winch with a 30 m long water hose
211 (4 mm inner diameter) attached. The CTD profiler with hose was lowered down continuously
212 at a constant speed (1 m min⁻¹). The exact depth and temperature of sampled water can be
213 extracted from the CTD profiler by correcting for the travel time of water sample flow in hose.
214 For the spatial mapping, a GPS antenna (Taoglas, AA.162, USA) was attached to the Picarro
215 gas analyzer. The water intake was submerged 0.5 m below the water surface together with the
216 CTD profiler and fixed to one side of the boat. The boat was driven at a constant speed of 5 km
217 h⁻¹.

218 **2.4 Theoretical background and data processing**

219 The FaRAGE shares a similar working principle to the Weiss-type gas equilibrator
220 described by Johnson (1999). The theoretical background and equations are provided in S3.

221 A simplified calculation is described by referring to the manual headspace method. In
222 principle the gas-water mixture is analogous to the static headspace method with the final gas
223 concentration in the gas phase assumed to reach a full equilibrium with that dissolved in the
224 aqueous phase. Therefore, by specifying the mixing ratio of air and water, the total mass of CH₄,
225 for instance, can be calculated by summing up the CH₄ in the headspace with the dissolved CH₄
226 (at equilibrium according to Henry's law, which is temperature and pressure dependent) in the
227 aqueous phase and subtracting the mass of background CH₄ (from the carrying gas with known
228 concentration). The dissolved gas concentration is then expressed as the volumetric
229 concentration of the total net mass of either CH₄ or CO₂ in the dissolved phase in the given
230 sample volume. A separated exemplary calculation sheet (excel file S5) is provided, which
231 allows for correction for temperature and pressure change (Goldenfum, 2010).

232 As the equilibration is only partially reached (< 92%), a correction coefficient is needed.
233 This can be obtained by measuring the water samples with known concentrations across a large
234 gradient. By referring to the results measured with the manual headspace method assuming full
235 equilibration (Magen et al., 2014), an equation for precise correction of the measured dissolved
236 gas concentrations can be obtained.

237 **3 Results and Discussion**

238 **3.1 Detection limit, equilibration ratio and response time**

239 The FaRAGE is capable of achieving a high gas equilibration ratio. We observed a high
240 correlation ($R^2 = 1.000$, $p < 0.01$) between the concentrations obtained using the headspace
241 method and those measured using the FaRAGE (Fig. 2a) across a wide range of dissolved CH₄

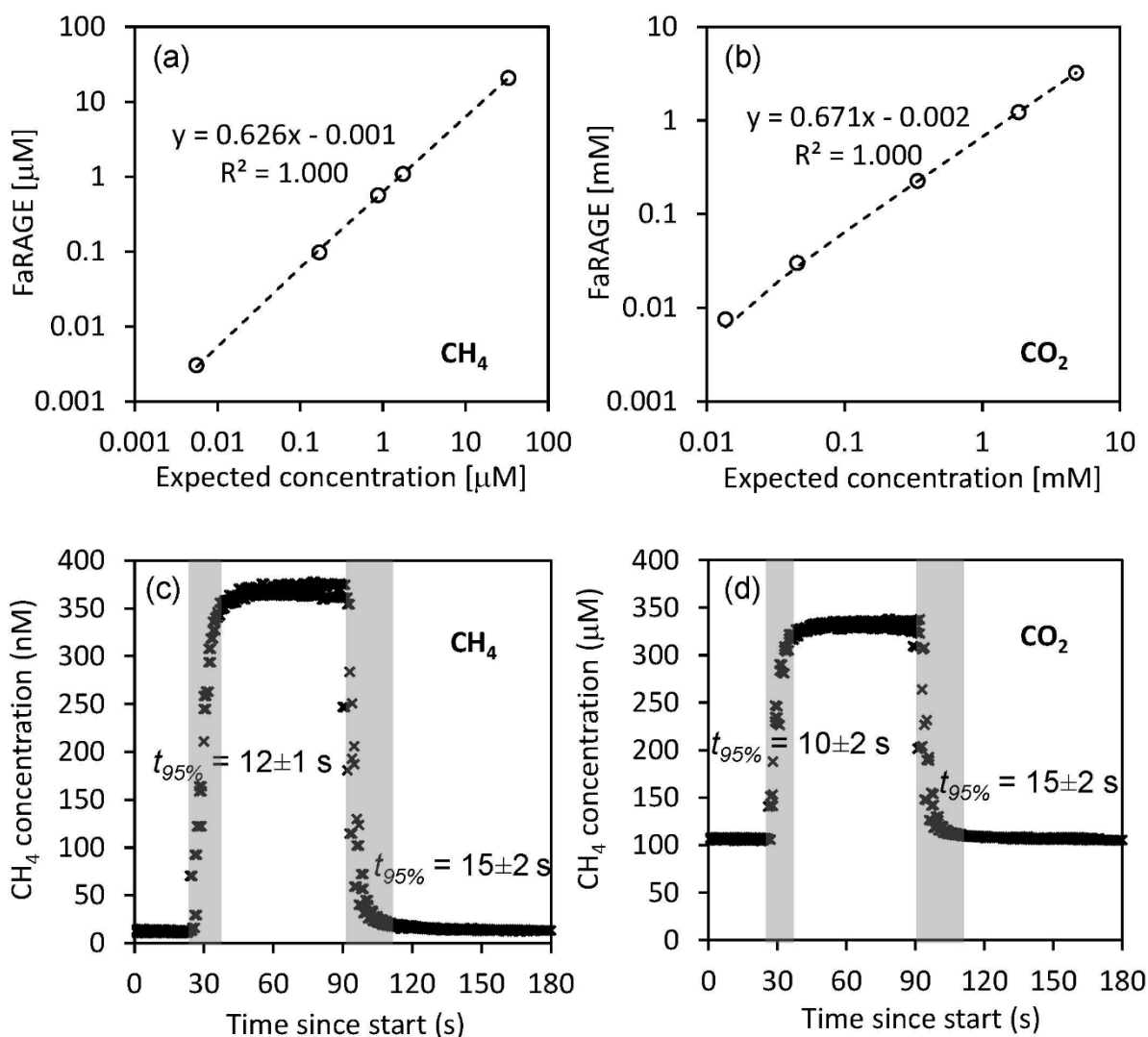
242 and CO₂ concentrations. The measurement accuracy is 0.5% (standard deviation in relation to
243 final concentration) once a stable plateau was reached (Fig. 2c). For CH₄, the FaRAGE reaches
244 a high equilibration ratio (62.6%) and ensures a rapid response. The determined response time
245 $t_{95\%}$ is only 12 ± 1 s when switching from low-to-high (nano-to-sub micro molar) dissolved CH₄
246 concentrations while the $t_{95\%}$ is a little longer (15 ± 2 s) when switching from high-to-low
247 concentration (Fig. 2c). For the current design specifications that allow for a high equilibration
248 ratio, the detection is theoretically limited by the sensitivity of the coupled gas analyzer. In the
249 lab tests, a clear response was observed at least for CH₄ concentration at air saturation (5.5 nM
250 inside the lab building). The measurable CH₄ concentrations should be at least sub-nM (10^{-10}
251 mol L⁻¹) given the high performance of cavity-ring-down gas analyzers. This is more than
252 sufficient for applications in inland waters where dissolved CH₄ concentrations are often above
253 air saturation. Despite CO₂ (Weiss, R. F., 1974) is an order of magnitude more soluble in water
254 than CH₄ (Wiesenburg and Guinasso, 1979), similar performances of the FaRAGE were
255 observed when measuring dissolved CO₂. An equilibration ratio of 67.1% (Fig. 2b) was
256 achieved with a fast response (Fig. 2d; $t_{95\%} = 10 \pm 2$ and 15 ± 2 for low-to-high and high-to-
257 low, respectively) when a 2 m mixing tube was used.

258 The response time for the FaRAGE results from two components: 1) the response of the
259 gas analyzer to changes in gas concentration and 2) the physical gas-water exchange process.
260 The response time for the gas analyzer is 5 s when the CH₄ concentration increases (Fig. S2).
261 The FaRAGE itself needs < 10 s to reach 95% of the final steady-state concentration.

262 Equilibration ratio and response time of the FaRAGE is not sensitive to the water-to-gas
263 mixing ratio (Fig. 3a) but rather to the length of the tube attached after the gas-water mixing
264 unit (Fig. 3c). A small effect, of the increased water-to-gas mixing ratio was also observed on
265 the equilibration ratio. The increased water-to-gas mixing ratio did not substantially change the
266 response time of the device (9.5 ± 1.5 s for low-to-high and 13.9 ± 2.4 s for high-to-low,

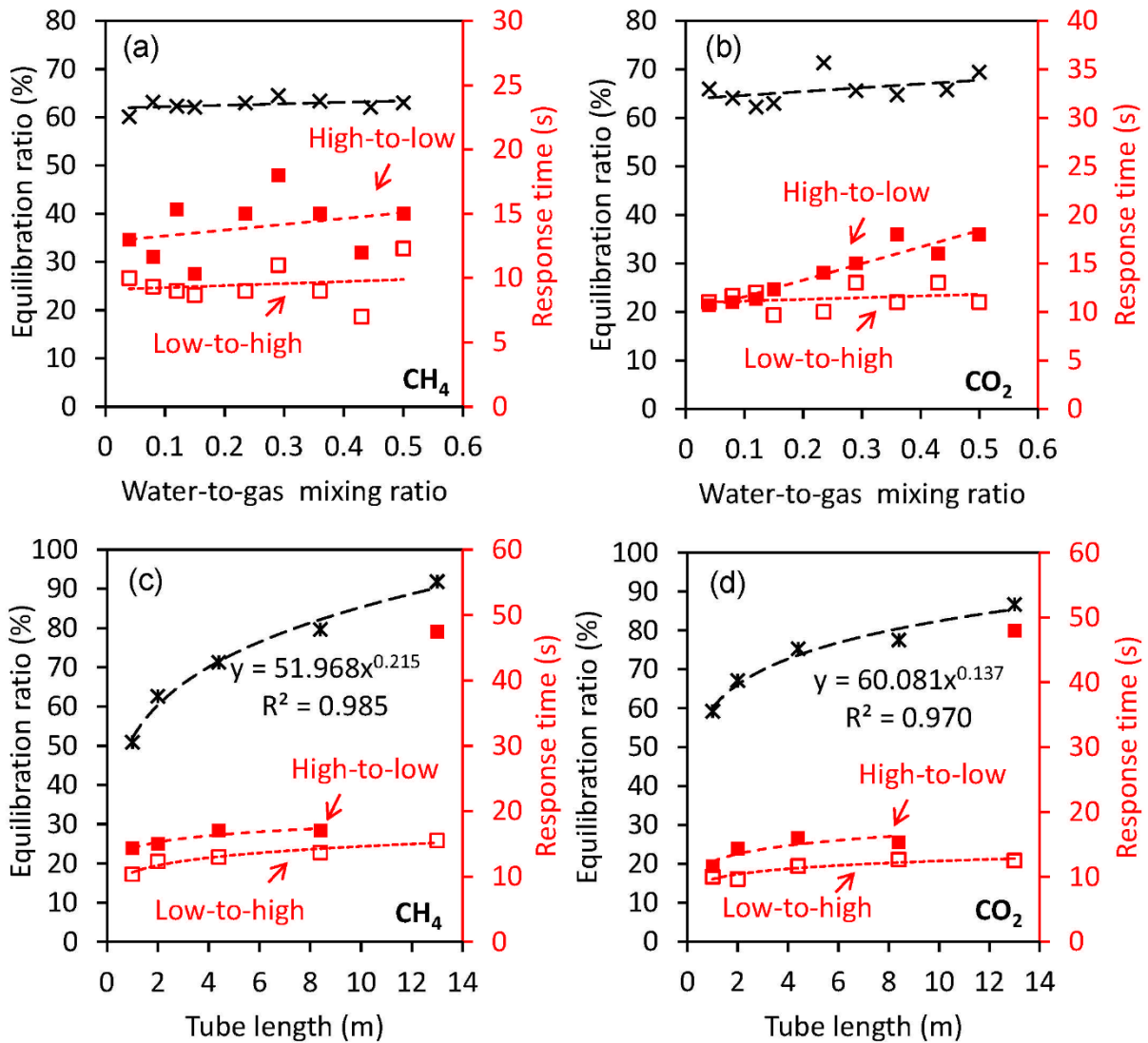
267 respectively). This is in contrast to other types of equilibrators in which an increase of water-
268 to-gas mixing ratio was found to result in a faster response (Webb et al., 2016). However, a
269 sharp enhancement of equilibration ratio was observed due to the extended length of the tube
270 for the gas-water mixing unit. A 91.8% equilibration ratio can be achieved by extending the
271 tube length to 13 m while extended response times are expected (low-to-high 17 s and high-to-
272 low 47.5 s, respectively). Increases in response time were notable when the tube-length
273 exceeded 13 m and were considered excessive at a tube length of 18 m (Fig 3c-d). Further
274 enhancement of the equilibration ratio was thus not possible when a longer tube (e.g. 18 m) was
275 used. The gas flow rate cannot be stabilized at 1 L min⁻¹ due to the increased resistance in
276 response to the further extension of tube length. Equilibration ratio and response time were
277 affected by the length of the tube after the gas-water mixing in a similar way as it was for CH₄
278 (Fig. 3b, d) with only one exception in the response time when the dissolved CO₂ concentration
279 changed from high to low. The response time increased linearly ($R^2 = 0.910$, $p < 0.01$) from 11
280 s to 18 s in response to the increase of water-to-gas ratio from 0.04 to 0.5.

281 As shown in Table S2 and Fig. S2, the fast response of the FaRAGE is partly due to the
282 extremely fast response of the Picarro Gas Scouter. Tests were performed by adapting the
283 FaRAGE to two other greenhouse gas analyzers (Ultraportable Los Gatos and Picarro G2132-
284 i) and the response times are listed in Table S3. Comparisons were made in Webb et al. (2016)
285 and Hartmann et al. (2018) where both CH₄ and ¹³δC-CH₄ were measured using a Picarro
286 G2201-i (Picarro, USA). Here we used a similar Picarro stable isotopic gas analyzer (Picarro
287 G2132-i) and unified all previous reported response times τ to $t_{95\%}$ by applying the equation $t_{95\%}$
288 = 3τ . The comparison between up-to-date previous studies and this study (Table S4)
289 demonstrated the extraordinary fast response relative to all existing gas equilibration devices.
290 A 53 s response time was achieved when the FaRAGE was adapted to the Picarro G2132-i,
291 which is substantially faster than previously reported (171-6744 s).



293

294 **Fig. 2** Performance of the Fast-Response Automated Gas Equilibrator (FaRAGE with a 2-m
 295 tube in the gas-water mixing unit) for both dissolved CH₄ and CO₂. (a)-(b) Correction equations
 296 for dissolved CH₄ and CO₂, respectively by referring FaRAGE measurements to expected
 297 concentrations measured using the manual headspace method. The dashed lines show a linear
 298 fit and the equations are shown next to the lines. Note that in the two graphs both axes are log
 299 transformed. (c)-(d) Exemplary response time of FaRAGE for low-to-high and high-to-low
 300 concentration changes (water-to-gas mixing ratio 0.5). Triplicated tests were performed and the
 301 average response time was taken at the time point when 95% of the final concentration was
 302 reached.



303

304 **Fig. 3** Factors affecting performance of the gas equilibrators for both dissolved CH₄ and CO₂.

305 (a)-(b) Equilibration ratio and response time in response to changing water/gas mixing ratio

306 (with a 2-m tube in the gas-water mixing unit). Black cross symbols are equilibration ratios,

307 and low-to-high and high-to-low response times are represented by red open and solid squares,

308 respectively. (c)-(d) Equilibration ratio and response time in response to changing tube length

309 of gas-water mixing unit (with a fixed water-to-gas mixing ratio of 0.5). Black cross symbols

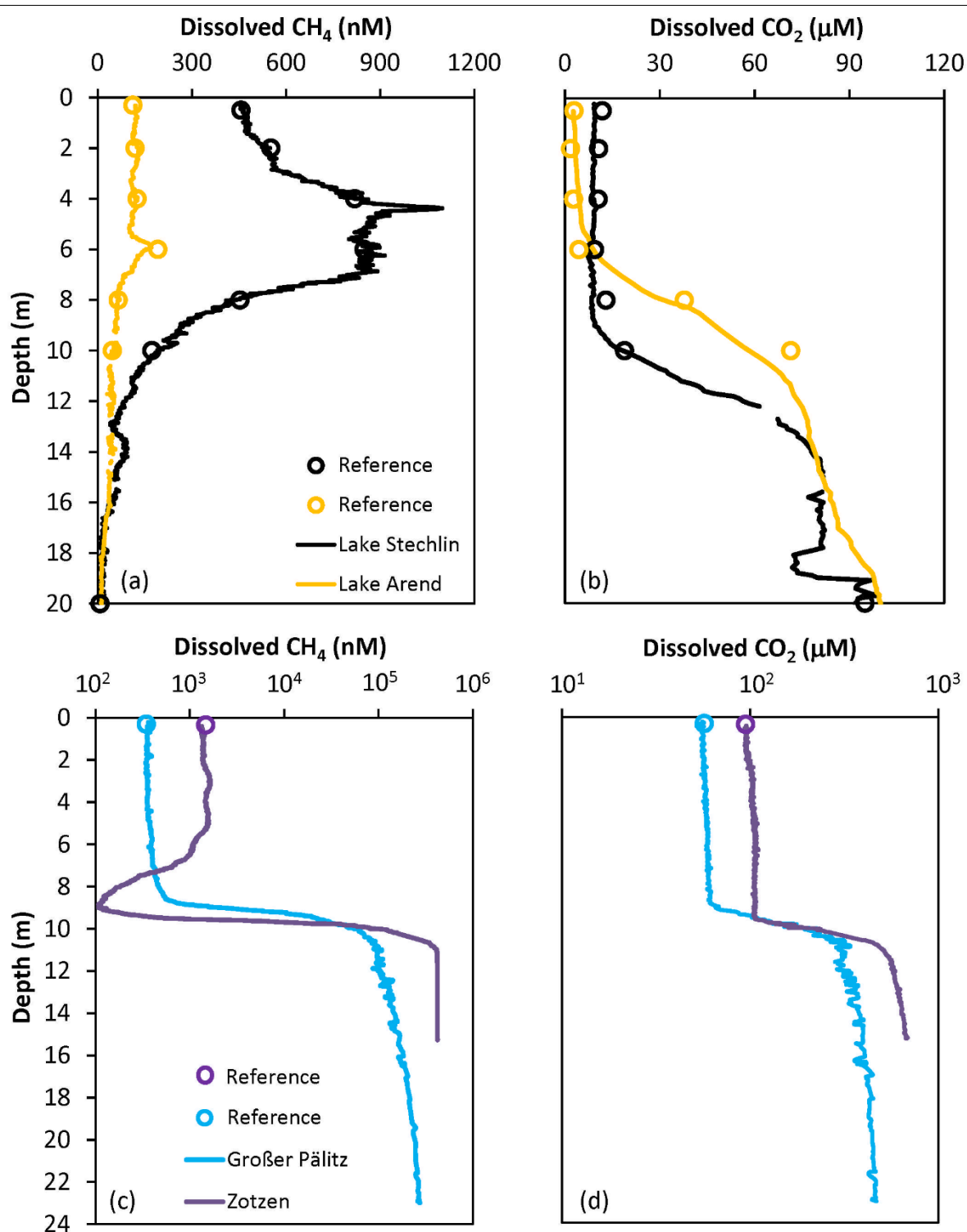
310 are equilibration ratios, and low-to-high and high-to-low response times are represented by red

311 open and solid squares, respectively.

312 **3.2 Depth profiles of dissolved CH₄ and CO₂ from multiple lakes**

313 Good agreement was observed between depths profiles of dissolved CH₄ and CO₂
314 concentration measured using the FaRAGE and the manual headspace method (Fig. 4). The
315 occurrence of a maximum in the vertical profile of dissolved CH₄ concentration in the upper
316 layer of Lake Stechlin (Fig. 4a) is consistent with previous observations (Grossart et al., 2011;
317 Tang et al., 2014; Hartmann et al., 2018). In Lake Arend we also observed a CH₄ peak (Fig. 4a)
318 although the overall concentration was lower. The opposite was observed at Lake Großer Pälitz
319 and Lake Zotzen (Fig. 4c) with an anoxic hypolimnion, where the dissolved CH₄ concentration
320 was three orders of magnitude higher than in the epilimnion. Higher dissolved CO₂ (10² - 10³
321 μM) was also observed in the hypolimnion of these two lakes (Fig. 4d) in comparison to Lake
322 Stechlin and Lake Arend (< 10² μM in Fig. 4b).

323 In contrast to the headspace method, the FaRAGE allowed for profiles of CH₄ and CO₂
324 to be described at a high vertical resolution, similar to that obtained with more sophisticated
325 membrane filter equilibrators (Hartmann et al., 2018; Gonzalez-Valencia et al., 2014). The
326 FaRAGE was capable of resolving differences in dissolved CH₄ and CO₂ concentrations in lake
327 water at decimeter resolution with ease. Whilst care should be taken to ensure the sampling
328 hose moves smoothly and slowly through the water column, continuous profiling of a 20 m
329 deep lake can be completed in 30 min. This is a big advantage since *in situ* CH₄ concentrations
330 can vary at very short time scales (hours to days) subject to internal production, oxidation,
331 weather conditions, etc. (cf. Hartmann et al. (2020)).



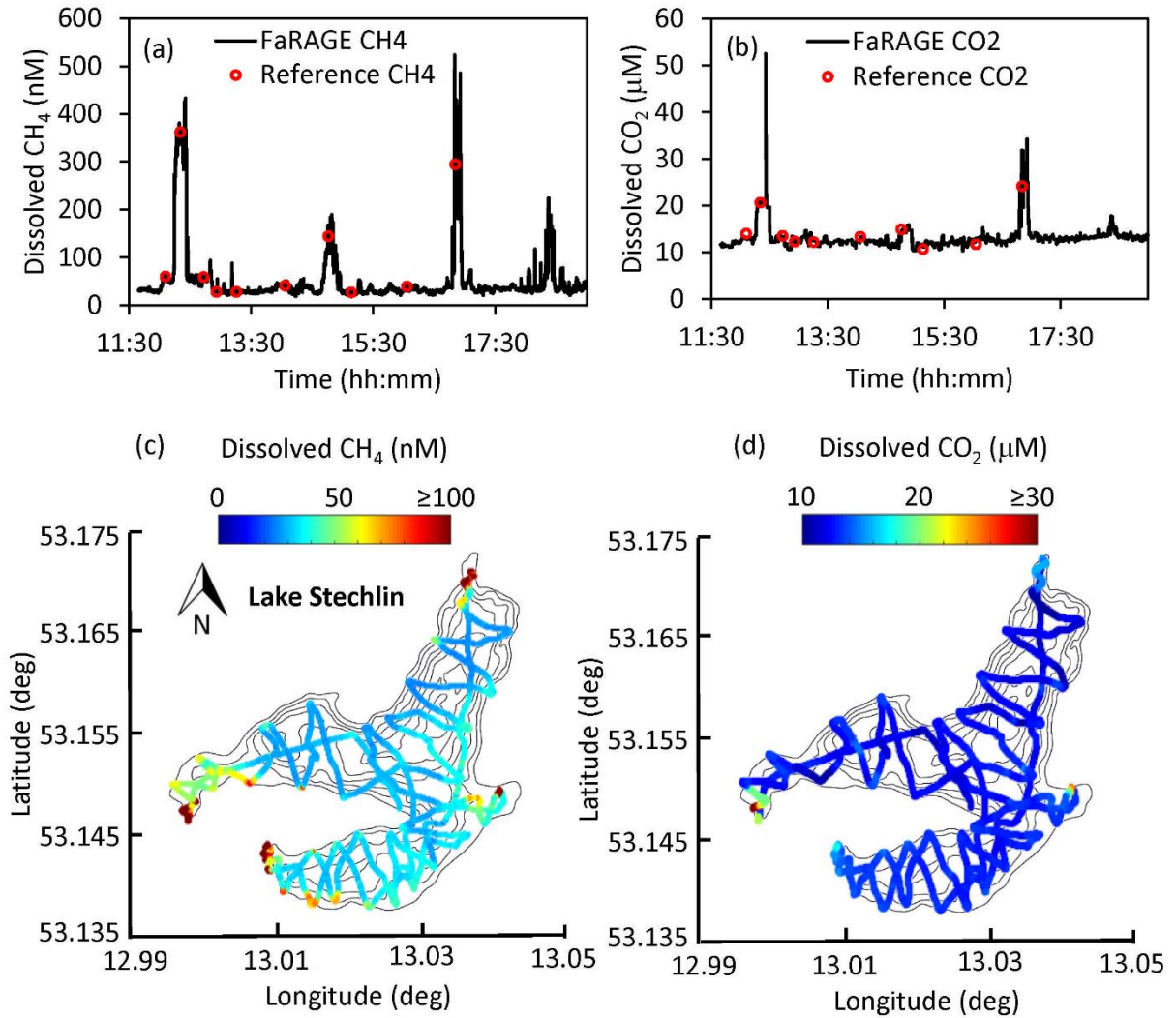
333

334 **Fig. 4** Depth profiles of dissolved CH₄ and CO₂ concentration from a set of lakes in Germany:
 335 (a)-(b) Lake Stechlin and Lake Arend with an oxygenated hypolimnion in summer; (c)-(d) Lake
 336 Großer Pälitz and Lake Zotzen, both with an anoxic hypolimnion in October. Note the log
 337 transformed x-axis is used in (c)-(d). References using the headspace method are designated as
 338 red open circles and measurements using the FaRAGE are shown as solid lines.

339 **3.3 Resolving spatial variability of dissolved CH₄ and CO₂ concentrations**

340 We confirmed the capability of the FaRAGE to operate continuously over a 7-h period
341 without notable decreases in performance (Fig. 5a-b). Benefitting from its fast response rate,
342 surface water dissolved CH₄ and CO₂ concentrations across the 4.52 km² Lake Stechlin were
343 mapped with great detail within one day (Fig. 5c-d). During the cruise, 10 reference
344 measurements were made at different sites and times, which were consistent with nonstop
345 online *in situ* measurements. The cruising survey demonstrated the capability of this device for
346 resolving not just vertical dynamics of CH₄ and CO₂ in lake water, but also the potential for
347 studying horizontal gas distributions across large distances, for instance large lakes and rivers.
348 With a driving speed of 5 km h⁻¹ and a response time of 12 s, a spatial resolution of 17 m can
349 be achieved, which is sufficient for such a medium-sized lake.

350



351

352 **Fig. 5** Map of surface dissolved CH₄ concentration at Lake Stechlin. (a)-(b) Time series of 7-h
 353 continuous surface water CH₄ and CO₂ measurement on March 28, 2019. The reference
 354 headspace measurements are shown as red circles. (c)-(d) Spatial distribution of surface water
 355 CH₄ and CO₂ concentration is given on top of the lake's bathymetry. Colored symbols show
 356 CH₄ and CO₂ concentrations according to the color bars. Black lines show the outline of the
 357 lake with depth contours.

358 4 Comments and Recommendations

359 4.1 Adaptability to different gas analyzers

360 The reasons for the significantly shortened response time of the FaRAGE compared to
361 other types of gas equilibrators are two-fold. While the working principle of the FaRAGE is
362 based on the bubble-type (Schneider et al., 1992) and Weiss-type equilibrators (Johnson, 1999),
363 a reduced headspace volume is adopted, which enhances the physical gas-water exchange.
364 Another reason is the use of an extremely fast-response gas analyzer (Picarro Gas Scouter 4301).
365 It is a highly recommended combination for measurement of dissolved gasses when the best
366 time-wise performance is preferred due to its great mobility (Table S2). However, coupling to
367 other Cavity-Ring-Down gas analyzers is also possible (Table S3). This feature enables a
368 possibility to investigate stable isotopic nature of dissolved CH₄ and CO₂, which is important
369 when sources of CH₄ and CO₂ need to be identified.

370 When a portable gas analyzer (Picarro Gas Scouter or Ultraportable Los Gatos) is used
371 for measuring CH₄ and CO₂ concentrations only, the gas equilibrator can be optimized for
372 different application environments. The length of coiled tube for gas-water mixing can be
373 adjusted to change the response time (Fig. 3c-d). For smaller lakes a higher spatial resolution
374 can be obtained by shortening the equilibration tubing, which shortens the response time, and
375 hence increases the spatial resolution, whilst maintaining an acceptable equilibration ratio (51%
376 when tube length is 1 m). In environments with extremely low dissolved CH₄ concentrations,
377 e.g. ocean waters, a longer gas-water mixing tube should be used to ensure a high gas
378 equilibration ratio.

379 To measure stable isotopic CH₄ and CO₂ in water, the sensitivity of the FaRAGE can be
380 modified to better adapt to the choice of gas analyzer. For example, high dissolved CH₄
381 concentrations (e.g. μM -to- mM range) can be measured with greater accuracy by increasing
382 the flow rate of the carrier gas relative to the sample water flow, therefore diluting the CH₄
383 concentrations to the range of the gas analyzer. This can be particularly useful, for instance,
384 when an instrument has an optimal precision at a low concentration range (1.8-12 ppm, e.g.,

385 Picarro G2201-i or G2132-i analyzers) for ^{13}C -CH₄ measurements. By using pure N₂ gas or
386 carrier gases (e.g. Helium and Argon) and corresponding gas analyzers, it would be possible to
387 measure other dissolved trace gas concentrations, e.g. N₂O.

388 **4.2 Uncertainties due to suspended solids, temperature and pressure change**

389 The FaRAGE is proven to be resistant to suspended solids in freshwater lakes without
390 having to use additional accessories. As shown in Fig. S3, apparent phytoplankton blooms were
391 observed in the two studied lakes each with a high biomass (Chl-a > 30 $\mu\text{g L}^{-1}$) in the epilimnetic
392 water. The measurements were unaffected, without any interruptions during measurements. As
393 algal particles are a large component of suspended particle concentration in lakes without high
394 suspended sediment concentration, it is safe to claim the resistance of this device to suspended
395 solids in such systems. However, care must be taken to avoid the water intake hose hitting the
396 bottom sediment, which could cause blockage of the water hose. An additional filtration unit
397 for the water intake might be needed when the device is to be applied to turbid rivers.

398 The temperature and hydrostatic pressure could both change when water is pumped out
399 through a water hose. To consider the temperature effect, a fast temperature logger is used (Fig.
400 1) which allows for corrections in calculation. Instead of using *in situ* lake temperature, the
401 temperature measured at the gas equilibrator, where gas equilibration occurs, should be used.
402 Our measurements found a minor effect when measuring surface waters but an apparent
403 warming for hypolimnetic water in deep lakes (Fig. S4).

404 The temperature correction can be made by referring to the manual headspace method.
405 The constant gas and water flow can be used as headspace and water volume, respectively. By
406 considering the temperature and pressure effects on gas solubility, the dissolved CH₄ and CO₂
407 concentrations can be calculated (an example calculation sheet is provided in Table S5). The
408 calibration curve can be established using the manual headspace measurements as standards.

409 The final concentrations can be corrected for partial equilibration by applying the equation from
410 the calibration curve (e.g., Fig. 2a-b). The response time should be deduced when calculating
411 CH₄ and CO₂ depth profiles and spatial distributions, in addition to the time lag caused by
412 pumping water samples by using an extended water intake hose.

413 **4.3 Calibration, maintenance and mobility**

414 The FaRAGE can be readily adopted for measuring other trace gases when coupled with
415 other portable gas analyzers. Due to differences in gas solubility (Duan and Sun, 2003;
416 Wiesenburg and Guinasso Jr, 1979), for each new gas, it would be necessary to establish the
417 relative equilibration efficiency and response time, following the approach we outlined here for
418 CH₄ and CO₂. Once set, a new calibration is only required when the tubing diameter or length
419 is changed (when the old one is no longer usable due to biofilm growth). This can be done by
420 referring to a number of known concentrations that covers a wide range (at least 5), e.g., taking
421 water samples from different water depth of the lake or a gradient from littoral to pelagic zones.
422 Once this full calibration is made, the calibration curve can be used for calculating the
423 subsequent measurements. A one-point reference measurement should be performed between
424 depth profiles or transects to check for apparent drifting. This can usually be done by taking
425 one surface water sample from a lake for manual headspace measurement. Care should be taken
426 when measuring in lakes with an anoxic hypolimnion where hydrogen sulfide is likely to
427 accumulate. The performance of Cavity-Ring-Down gas analyzers can be potentially affected
428 by H₂S (Kohl et al., 2019). At these sites, it is recommended to use a copper scrubber to remove
429 H₂S from the gas samples (Malowany et al. 2015) and no time delay will be induced.

430 The gas equilibrators should be carefully maintained. Replacement of parts is
431 recommended at a monthly basis provided the device is heavily in use. They include bubble
432 diffusor and the coiled gas-water mixing tube. In addition, to ensure the performance and
433 prevent biofilm formation the gas-water mixing and separation units should be cleaned after

434 use. Running with distilled or Milli-Q water would help to rinse the device and reduce the risk
435 of biofilm development in the inner tubes. The performance of peristaltic pumps should be also
436 regularly checked and the inner pump tubes need to be replaced to ensure a constant water flow.

437 The combination of FaRAGE with the Picarro Gas Scouter provides the most mobility.
438 The system can be easily carried by one person and work in a small aluminum or inflatable boat
439 where a maximum capacity of three people is possible. The device can also work in bad weather
440 with additional measures based on protecting the gas analyzer from water damage by rain or
441 flooding.

442 **Code availability**

443 Not applicable.

444 **Data Availability**

445 An example calculation sheet (raw data of Fig. 2a) is provided as part of supporting
446 information for device calibration and for temperature and pressure correction when calculating
447 dissolved methane concentration. The full data sets associated with lab and field tests are
448 available upon request.

449 **Supplement link**

450 From Copernicus.

451 **Author contributions**

452 SBX and WW proposed the idea and built the first prototype. LL improved the prototype
453 and conducted lab and field tests. JW contributed to the field tests. AL contributed to the
454 derivation of equations; HPG led the project and advised the development of the modified

455 prototype. LL drafted the initial manuscript. All authors discussed the results and commented
456 on the manuscript.

457 **Competing interests**

458 The authors declare that they have no conflict of interest.

459 **Acknowledgements**

460 This work was financially supported by the National Natural Science Foundation of
461 China (grant No. 51979148 & 91647207). L.L., J.W. and H.P.G. were financially supported by
462 the “Aquameth” project of the German Research Foundation (DFG GR1540/21-1+2). We thank
463 Andreas Jechow, Christine Kiel, Igor Ogashawara, Katrin Kohnert, Sabine Wollrab and Stella
464 Berger for providing support with collecting field test data under project CONNECT (SAW-
465 K45/2017) which is funded by the Leibniz Association, Germany. The authors would like to
466 thank Hannah Geisinger and Truls Hveem Hansson for helping collecting field data.

467 **References**

- 468 Bastviken, D., Cole, J., Pace, M., and Tranvik, L.: Methane emissions from lakes:
469 Dependence of lake characteristics, two regional assessments, and a global estimate, *Global*
470 *Biogeochem. Cy.*, 18, <https://doi.org/10.1029/2004GB002238>, 2004.
- 471 Bastviken, D., Tranvik, L. J., Downing, J. A., Crill, P. M., and Enrich-Prast, A.: Freshwater
472 methane emissions offset the continental carbon sink, *Science*, 331, 50-50,
473 <https://doi.org/10.1126/science.1196808>, 2011.
- 474 Bižić, M., Klintzsch, T., Ionescu, D., Hindiyeh, M. Y., Günthel, M., Muro-Pastor, A. M.,
475 Eckert, W., Urich, T., Keppler, F., and Grossart, H.-P.: Aquatic and terrestrial cyanobacteria
476 produce methane, *Sci. Adv.*, 6, eaax5343, <https://doi.org/10.1126/sciadv.aax5343>, 2020.

477 Boulart, C., Connelly, D., and Mowlem, M.: Sensors and technologies for in situ dissolved
478 methane measurements and their evaluation using Technology Readiness Levels, Trends
479 Anal. Chem., 29, 186-195, <https://doi.org/10.1016/j.trac.2009.12.001>, 2010.

480 Cole, J. J., Prairie, Y. T., Caraco, N. F., McDowell, W. H., Tranvik, L. J., Striegl, R. G.,
481 Duarte, C. M., Kortelainen, P., Downing, J. A., and Middelburg, J. J.: Plumbing the global
482 carbon cycle: integrating inland waters into the terrestrial carbon budget, Ecosystems, 10,
483 172-185, <https://doi.org/10.1007/s10021-006-9013-8>, 2007.

484 Donis, D., Flury, S., Stöckli, A., Spangenberg, J. E., Vachon, D., and McGinnis, D. F.: Full-
485 scale evaluation of methane production under oxic conditions in a mesotrophic lake, Nat.
486 Commun., 8, 1661, <https://doi.org/10.1038/s41467-017-01648-4>, 2017.

487 Duan, Z., and Sun, R.: An improved model calculating CO₂ solubility in pure water and
488 aqueous NaCl solutions from 273 to 533 K and from 0 to 2000 bar, Chem. Geol., 193, 257-
489 271, [https://doi.org/10.1016/S0009-2541\(02\)00263-2](https://doi.org/10.1016/S0009-2541(02)00263-2), 2003.

490 Encinas Fernández, J., Peeters, F., and Hofmann, H.: Importance of the autumn overturn and
491 anoxic conditions in the hypolimnion for the annual methane emissions from a temperate
492 lake, Environ. Sci. Technol., 48, 7297-7304, <https://doi.org/10.1021/es4056164>, 2014.

493 Fernández, J. E., Peeters, F., and Hofmann, H.: On the methane paradox: Transport from
494 shallow water zones rather than in situ methanogenesis is the major source of CH₄ in the open
495 surface water of lakes, J. Geophys. Res.: Biogeosciences, 121, 2717-2726,
496 <https://doi.org/10.1002/2016JG003586>, 2016.

497 Frankignoulle, M., Borges, A., and Biondo, R.: A new design of equilibrators to monitor
498 carbon dioxide in highly dynamic and turbid environments, Water Res., 35, 1344-1347,
499 [https://doi.org/10.1016/S0043-1354\(00\)00369-9](https://doi.org/10.1016/S0043-1354(00)00369-9), 2001.

500 Goldenfum, J. A.: GHG Measurement Guidelines for Freshwater Reservoirs, UNESCO/IHA,
501 London, UK, 139 pp., 2010.

502 Gonzalez-Valencia, R., Magana-Rodriguez, F., Gerardo-Nieto, O., Sepulveda-Jauregui, A.,
503 Martinez-Cruz, K., Walter Anthony, K., Baer, D., and Thalasso, F.: In situ measurement of
504 dissolved methane and carbon dioxide in freshwater ecosystems by off-axis integrated cavity
505 output spectroscopy, *Environ. Sci. Technol.*, 48, 11421-11428,
506 <https://doi.org/10.1021/es500987j>, 2014.

507 Grossart, H.-P., Frindte, K., Dziallas, C., Eckert, W., and Tang, K. W.: Microbial methane
508 production in oxygenated water column of an oligotrophic lake, *Proc. Natl. Acad. Sci.*, 108,
509 19657-19661, <https://doi.org/10.1073/pnas.1110716108>, 2011.

510 Gülzow, W., Rehder, G., Schneider, B., Deimling, J. S. v., and Sadkowiak, B.: A new method
511 for continuous measurement of methane and carbon dioxide in surface waters using off-axis
512 integrated cavity output spectroscopy (ICOS): An example from the Baltic Sea, *Limnol.*
513 *Oceanogr.: Methods*, 9, 176-184, <https://doi.org/10.4319/lom.2011.9.176>, 2011.

514 Günthel, M., Donis, D., Kirillin, G., Ionescu, D., Bizic, M., McGinnis, D. F., Grossart, H.-P.,
515 and Tang, K. W.: Contribution of oxic methane production to surface methane emission in
516 lakes and its global importance, *Nat. Commun.*, 10, 1-10, [https://doi.org/10.1038/s41467-019-](https://doi.org/10.1038/s41467-019-13320-0)
517 [13320-0](https://doi.org/10.1038/s41467-019-13320-0), 2019.

518 Hartmann, J. F., Gentz, T., Schiller, A., Greule, M., Grossart, H. P., Ionescu, D., Keppler, F.,
519 Martinez-Cruz, K., Sepulveda-Jauregui, A., and Isenbeck-Schröter, M.: A fast and sensitive
520 method for the continuous in situ determination of dissolved methane and its $\delta^{13}\text{C}$ -isotope
521 ratio in surface waters, *Limnol. Oceanogr.: Methods*, 16, 273-285,
522 <https://doi.org/10.1002/lom3.10244>, 2018.

523 Hartmann, J. F., Gunthel, M., Klintzsch, T., Kirillin, G., Grossart, H.-P., Keppler, F., and
524 Isenbeck-Schröter, M.: High Spatio-Temporal Dynamics of Methane Production and
525 Emission in Oxic Surface Water, *Environ. Sci. Technol.*, 54, 1451-1463,
526 <https://doi.org/10.1021/acs.est.9b03182>, 2020.

527 Hofmann, H., Federwisch, L., and Peeters, F.: Wave-induced release of methane: Littoral
528 zones as source of methane in lakes, *Limnol. Oceanogr.*, 55, 1990-2000,
529 <https://doi.org/10.4319/lo.2010.55.5.1990>, 2010.

530 Hofmann, H.: Spatiotemporal distribution patterns of dissolved methane in lakes: How
531 accurate are the current estimations of the diffusive flux path?, *Geophys. Res. Lett.*, 40, 2779-
532 2784, <https://doi.org/10.1002/grl.50453>, 2013.

533 Johnson, J. E.: Evaluation of a seawater equilibrators for shipboard analysis of dissolved
534 oceanic trace gases, *Anal. Chim. Acta*, 395, 119-132, [https://doi.org/10.1016/S0003-](https://doi.org/10.1016/S0003-2670(99)00361-X)
535 [2670\(99\)00361-X](https://doi.org/10.1016/S0003-2670(99)00361-X), 1999.

536 Juutinen, S., Rantakari, M., Kortelainen, P., Huttunen, J. T., Larmola, T., Alm, J., Silvola, J.,
537 and Martikainen, P. J.: Methane dynamics in different boreal lake types, *Biogeosciences*, 6,
538 209–223, <https://doi.org/10.5194/bg-6-209-2009>, 2009.

539 Kohl, L., Koskinen, M., Rissanen, K., Haikarainen, I., Polvinen, T., Hellén, H., and Pihlatie,
540 M.: Interferences of volatile organic compounds (VOCs) on methane concentration
541 measurements, *Biogeosciences*, 16, 3319-3332, <https://doi.org/10.5194/bg-16-3319-2019>,
542 2019.

543 Körtzinger, A., Thomas, H., Schneider, B., Gronau, N., Mintrop, L., and Duinker, J. C.: At-
544 sea intercomparison of two newly designed underway pCO₂ systems - encouraging results,
545 *Mar. Chem.*, 52, 133-145, [https://doi.org/10.1016/0304-4203\(95\)00083-6](https://doi.org/10.1016/0304-4203(95)00083-6), 1996.

546 Kreling, J., Bravidor, J., Engelhardt, C., Hupfer, M., Koschorreck, M., and Lorke, A.: The
547 importance of physical transport and oxygen consumption for the development of a
548 metalimnetic oxygen minimum in a lake, *Limnol. Oceanogr.*, 62, 348-363,
549 <https://doi.org/10.1002/lno.10430>, 2017.

550 Li, Y., Zhan, L., Zhang, J., and Chen, L.: Equilibrator-based measurements of dissolved
551 methane in the surface ocean using an integrated cavity output laser absorption spectrometer,
552 *Acta Oceanol. Sin.*, 34, 34-41, <https://doi.org/10.1007/s13131-015-0685-9>, 2015.

553 Liu, R., Hofmann, A., Gülaçar, F. O., Favarger, P.-Y., and Dominik, J.: Methane
554 concentration profiles in a lake with a permanently anoxic hypolimnion (Lake Lugano,
555 Switzerland-Italy), *Chem. Geol.*, 133, 201-209, [https://doi.org/10.1016/S0009-](https://doi.org/10.1016/S0009-2541(96)00090-3)
556 2541(96)00090-3, 1996.

557 Magen, C., Lapham, L. L., Pohlman, J. W., Marshall, K., Bosman, S., Casso, M., and
558 Chanton, J. P.: A simple headspace equilibration method for measuring dissolved methane,
559 *Limnol. Oceanogr.: Methods*, 12, 637-650, <https://doi.org/10.4319/lom.2014.12.637>, 2014.

560 Murase, J., Sakai, Y., Sugimoto, A., Okubo, K., and Sakamoto, M.: Sources of dissolved
561 methane in Lake Biwa, *Limnology*, 4, 91-99, <https://doi.org/10.1007/s10201-003-0095-0>,
562 2003.

563 Malowany, K., Stix, J., Van Pelt, A., and Lucic, G.: H₂S interference on CO₂ isotopic
564 measurements using a Picarro G1101-i cavity ring-down spectrometer, *Atmos. Meas. Tech.*,
565 8, 4075-4082, <https://doi.org/10.5194/amt-8-4075-2015>, 2015.

566 Murase, J., Sakai, Y., Kametani, A., and Sugimoto, A.: Dynamics of methane in mesotrophic
567 Lake Biwa, Japan, *Ecol. Res.* 20, 377-385, <https://doi.org/10.1007/s11284-005-0053-x>, 2005.

568 Paranaíba, J. R., Barros, N., Mendonça, R., Linkhorst, A., Isidorova, A., Roland, F. b.,
569 Almeida, R. M., and Sobek, S.: Spatially resolved measurements of CO₂ and CH₄
570 concentration and gas-exchange velocity highly influence carbon-emission estimates of
571 reservoirs, *Environ. Sci. Technol.*, 52, 607-615, <https://doi.org/10.1021/acs.est.7b05138>,
572 2018.

573 Peeters, F., Fernandez, J. E., and Hofmann, H.: Sediment fluxes rather than oxic
574 methanogenesis explain diffusive CH₄ emissions from lakes and reservoirs, *Sci. Rep.*, 9,
575 <https://doi.org/10.1038/s41598-018-36530-w>, 2019.

576 Read, J. S., Hamilton, D. P., Desai, A. R., Rose, K. C., MacIntyre, S., Lenters, J. D., Smyth,
577 R. L., Hanson, P. C., Cole, J. J., and Staehr, P. A.: Lake-size dependency of wind shear and

578 convection as controls on gas exchange, *Geophys. Res. Lett.*, 39,
579 <https://doi.org/10.1029/2012GL051886>, 2012.

580 Rhee, T., Kettle, A., and Andreae, M.: Methane and nitrous oxide emissions from the ocean:
581 A reassessment using basin-wide observations in the Atlantic, *J. Geophys. Res.: Atmospheres*,
582 114, <https://doi.org/10.1029/2008JD011662>, 2009.

583 Santos, I. R., Maher, D. T., and Eyre, B. D.: Coupling automated radon and carbon dioxide
584 measurements in coastal waters, *Environ. Sci. Technol.*, 46, 7685-7691,
585 <https://doi.org/10.1021/es301961b>, 2012.

586 Saunio, M., Stavert, A. R., Poulter, B., et al.: The Global Methane Budget 2000–2017, *Earth*
587 *Syst. Sci. Data Discuss.*, <https://doi.org/10.5194/essd-2019-128>, in review, 2019.

588 Schlüter, M., and Gentz, T.: Application of membrane inlet mass spectrometry for online and
589 in situ analysis of methane in aquatic environments, *J. Am. Soc. Mass Spectrom.*, 19, 1395-
590 1402, <https://doi.org/10.1016/j.jasms.2008.07.021>, 2008.

591 Schneider, B., Kremling, K., and Duinker, J. C.: CO₂ partial pressure in Northeast Atlantic
592 and adjacent shelf waters: Processes and seasonal variability, *J. Marine Syst.*, 3, 453-463,
593 [https://doi.org/10.1016/0924-7963\(92\)90016-2](https://doi.org/10.1016/0924-7963(92)90016-2), 1992.

594 Stepanenko, V., Mammarella, I., Ojala, A., Miettinen, H., Lykosov, V., and Vesala, T.: LAKE
595 2.0: a model for temperature, methane, carbon dioxide and oxygen dynamics in lakes, *Geosci.*
596 *Model Dev.*, 9, 1977-2006, <https://doi.org/10.5194/gmd-9-1977-2016>, 2016.

597 Tang, K. W., McGinnis, D. F., Frindte, K., Brüchert, V., and Grossart, H.-P.: Paradox
598 reconsidered: Methane oversaturation in well-oxygenated lake waters, *Limnol. Oceanogr.*, 59,
599 275-284, <https://doi.org/10.4319/lo.2014.59.1.0275>, 2014.

600 Tranvik, L. J., Downing, J. A., Cotner, J. B., Loiselle, S. A., Striegl, R. G., Ballatore, T. J.,
601 Dillon, P., Finlay, K., Fortino, K., and Knoll, L. B.: Lakes and reservoirs as regulators of
602 carbon cycling and climate, *Limnol. Oceanogr.*, 54, 2298-2314,
603 https://doi.org/10.4319/lo.2009.54.6_part_2.2298, 2009.

604 Vachon, D., and Prairie, Y. T.: The ecosystem size and shape dependence of gas transfer
605 velocity versus wind speed relationships in lakes, *Can. J. Fish. Aquat. Sci.*, 70, 1757-1764,
606 <https://doi.org/10.1139/cjfas-2013-0241>, 2013.

607 Webb, J. R., Maher, D. T., and Santos, I. R.: Automated, in situ measurements of dissolved
608 CO₂, CH₄, and $\delta^{13}\text{C}$ values using cavity enhanced laser absorption spectrometry: Comparing
609 response times of air-water equilibrators, *Limnol. Oceanogr.: Methods*, 14, 323-337,
610 <https://doi.org/10.1002/lom3.10092>, 2016.

611 Weiss R.F.: Carbon dioxide in water and seawater: the solubility of a non-ideal gas, *Mar.*
612 *Chem.* 2, 203-215, [https://doi.org/10.1016/0304-4203\(74\)90015-2](https://doi.org/10.1016/0304-4203(74)90015-2), 1974.

613 Wiesenburg, D. A., and Guinasso Jr, N. L.: Equilibrium solubilities of methane, carbon
614 monoxide, and hydrogen in water and sea water, *J. Chem. Eng. Data*, 24, 356-360,
615 <https://doi.org/10.1021/je60083a006>, 1979.

616 Zimmermann M., Mayr M. J., Bouffard D., Eugster W., Steinsberger T., Wehrli B., Brand A.,
617 and Bürgmann H.: Lake overturn as a key driver for methane oxidation, *bioRxiv*,
618 <https://doi.org/10.1101/689182>, 2019.